# Calmodulin-dependent activation of the epithelial calcium-dependent chloride channel TMEM16A

**Yuemin Tian,* Patthara Kongsuphol,* Martin Hug,‡ Jiraporn Ousingsawat,* Ralph Witzgall,† Rainer Schreiber,*,[1] and Karl Kunzelmann*,[1,2]**

*Institut für Physiologie and †Institut für Anatomie, Universität Regensburg, Regensburg, Germany; and ‡Apotheke der Universitätsklinik Freiburg, Freiburg, Germany

ABSTRACT **TMEM16A (anoctamin 1, Ano1), a member of a family of 10 homologous proteins, has been shown to form an essential component of $Ca^{2+}$-activated $Cl^-$ channels. TMEM16A-null mice exhibit severe defects in epithelial transport along with tracheomalacia and death within 1 mo after birth. Despite its outstanding physiological significance, the mechanisms for activation of TMEM16A remain obscure. TMEM16A is activated on increase in intracellular $Ca^{2+}$, but it is unclear whether $Ca^{2+}$ binds directly to the channel or whether additional components are required. We demonstrate that TMEM16A is strictly membrane localized and requires cytoskeletal interactions to be fully activated. Despite the need for cytosolic ATP for full activation, phosphorylation by protein kinases is not required. In contrast, the $Ca^{2+}$ binding protein calmodulin appears indispensable and interacts physically with TMEM16A. Openers of small- and intermediate-conductance $Ca^{2+}$-activated potassium channels known to interact with calmodulin, such as 1-EBIO, DCEBIO, or riluzole, also activated TMEM16A. These results reinforce the use of these compounds for activation of electrolyte secretion in diseases such as cystic fibrosis.—Tian, Y., Kongsuphol, P., Hug, M., Ousingsawat, J., Witzgall, R., Schreiber, R., Kunzelmann, K. Calmodulin-dependent activation of the epithelial calcium-dependent chloride channel TMEM16A. *FASEB J.* 25, 1058–1068 (2011). www.fasebj.org**

*Key Words: $Ca^{2+}$-activated $Cl^-$ channels · anoctamin 1 · exocytosis · SK4 · 1-EBIO · cystic fibrosis*

BROADLY EXPRESSED $Ca^{2+}$-ACTIVATED $Cl^-$ channels (CaCCs) are of fundamental importance in many tissues, as they control electrolyte secretion, neuronal excitability, and smooth muscle contraction. CaCCs have been identified as TMEM16A (1–3). TMEM16A (anoctamin 1, ANO1) belongs to a family of 10 TMEM16-proteins (TMEM16A-K, ANO 1–10). TMEM16A has 8 putative transmembrane domains (TMDs) and a p-loop between TMD 5 and TMD 6. Along with multiple splice variants, several isoforms are coexpressed in a tissue-specific manner, which provides a $Ca^{2+}$-activated $Cl^-$ conductance of distinct biophysical and pharmacological features (4, 5). It has been shown that alternative splicing of TMEM16A changes voltage dependence and $Ca^{2+}$ sensitivity (4). Moreover, membrane expression, time dependence and amplitude of the current, $Ca^{2+}$ dependence, and sensitivity toward inhibitors vary among TMEM16 proteins. Preliminary data suggest that these proteins can exist as heterooligomeric complexes (6).

TMEM16A shows common characteristics of the native CaCCs, present in a large number of tissues and cell types (1–3, 7, 8). We and others demonstrated the fundamental importance of TMEM16A for $Ca^{2+}$-dependent $Cl^-$ secretion in a number of epithelial tissues (9–11). TMEM16A is essential for $Ca^{2+}$-dependent $Cl^-$ currents in airways, large intestine, salivary gland, pancreatic gland, and hepatocytes (9–11). Severe transport defects were detected in epithelial tissues of TMEM16A-knockout mice, leading to reduced saliva production and attenuated mucociliary clearance of the airways (9, 10, 12). Thus, TMEM16A is essential for proper development and hydration of the airways (13). Knockout animals die early because of unstable airways and because they cannot digest and absorb food. The outstanding physiological significance of TMEM16A is further supported by its role in pacemaker cells, where it controls smooth muscle contraction, and by its contribution to generation of acute nociceptive signals (3, 14–17). Moreover, TMEM16A does also participate in fundamental cellular mechanisms, such as regulation of the cell volume, and it interferes with *Escherichia coli* α-hemolysin-induced shrinkage of erythrocytes and subsequent hemolysis (18, 19).

Although it is clear that TMEM16A produces $Cl^-$ currents on increase in $[Ca^{2+}]i$, it is not known whether $[Ca^{2+}]i$ binds directly to the channel. A string of negatively charged glutamic acid residues in the first intracellular loop could form a $Ca^{2+}$ binding pocket, but its role for $Ca^{2+}$ binding remains unclear (20). The available data do not explain the mechanism for activation of TMEM16A by $Ca^{2+}$ and whether phosphorylation or membrane trafficking is required. Here, we elucidated the mechanisms for activation of TMEM16A and found that both ATP and calmodulin are required. The present results suggest a regulation of TMEM16A similar to that of

[1] These authors contributed equally to this work.

[2] Correspondence: Institut für Physiologie, Universität Regensburg, Universitätsstraße 31, D-93053 Regensburg, Germany. E-mail: karl.kunzelmann@vkl.uni-regensburg.de

doi: 10.1096/fj.10-166884

This article includes supplemental data. Please visit *http://www.fasebj.org* to obtain this information.



0892-6638/11/0025-1058 © FASEB

$Ca^{2+}$-activated $K^+$ (SK) channels. Also, both types of channels share pharmacological properties (21). Understanding the regulation of TMEM16A will allow the development of novel classes of pharmaceutical compounds, such as benzimidazolinones. Because both $Ca^{2+}$-dependent $K^+$ and $Cl^-$ channels are expressed in human airways, in contrast to adult human colon, which does not express $Ca^{2+}$-activated $Cl^-$ channels, benzimidazolinones are promising tools to reinstall $Cl^-$ secretion in airways in cystic fibrosis (CF).

## MATERIALS AND METHODS

### Cell culture, cDNAs, and transfection

HEK 293 and Calu-3 cells were grown in DMEM (Gibco, Karlsruhe, Germany) supplemented with 10% FBS at 37°C in a humidified atmosphere with 5% $CO_2$. Cells were plated on fibronectin- and collagen-coated coverslips and cotransfected with cDNA encoding either mTMEM16A, hTMEM16A, hSK4, or empty pcDNA3.1 vector (mock) along with $P2Y_2$ receptor and CD8. Transfections were carried out using Lipofectamine 2000 (Invitrogen, Karlsruhe, Germany) according to the manufacturer's protocol.

### Patch clamping

At 2 or 3 d after transfection, transfected cells were identified by incubating the cells 1–2 min with Dynabeads CD8 (Invitrogen). Coverslips were mounted on the stage of an inverted microscope (IM35; Carl Zeiss, Jena, Germany) and kept at 37°C. The bath was perfused continuously with Ringer solution at the rate of 5 ml/min. For fast whole-cell patch clamping, pipettes were filled with intracellular-like "physiological" solution containing 30 mM KCl, 95 mM potassium gluconate, 1.2 mM $NaH_2PO_4$, 4.8 mM $Na_2HPO_4$, 1 mM EGTA, 0.758 mM calcium gluconate, 1.034 mM $MgCl_2$, 5 mM D-glucose, and 3 mM ATP (pH 7.2), with an input resistance of 2–4 MΩ. Experiments were conducted as described earlier (9).

### Ussing chamber experiments

After isolation, mouse tracheas were immediately put into ice-cold buffer solution. Tracheas were opened longitudinally and mounted into a perfused micro-Ussing chamber with a circular aperture and a diameter of 0.95 mm. Luminal and basolateral sides of the epithelium were perfused continuously at a rate of 5 ml/min with solution containing 145 mM NaCl, 0.4 mM $KH_2PO_4$, 1.6 mM $K_2HPO_4$, 5 mM D-glucose, 1 mM $MgCl_2$, 5 mM HEPES, and 1.3 mM Ca gluconate (pH 7.4) that was heated to 37°C. Experiments were carried out under open-circuit conditions. Values for transepithelial voltages ($V_{te}$) were referred to the serosal side of the epithelium. Transepithelial resistance ($R_{te}$) was determined by applying short (1 s) current pulses ($\Delta I = 0.5$ μA) and after subtracting the resistance of the empty chamber using Ohm's law.

### ReAsH labeling and electron microscopy

HEK293 or COS-7 cells were transiently transfected using DEAE dextran/chloroquine (22). After 3 d, cells were incubated for 1 h at 37°C with 450 nM resorufin arsenical hairpin binding reagent (ReAsH; Invitrogen) and 12.5 μM 1,2-ethanedithiol (EDT; Fluka, Buchs, Switzerland); the cells were then washed twice briefly with 500 nM 2,3-dimercapto-1-propanol (BAL; Fluka), incubated in 500 nM BAL for 20 min at 37°C, washed again 3 times with HBSS, and fixed with 2% glutaraldehyde overnight. Cells were blocked for 30 min in 50 mM glycine, 10 mM KCN, 20 mM aminotriazole, and 0.001% $H_2O_2$, and were washed with new buffer containing 1 mg/ml of diaminobenzidine. Photoconversion was performed by exposing the cells at 4°C to a 585-nm light source. Finally, the cells were washed again and embedded in Durcupan (Fluka). Thin sections (50 nm) were analyzed in a Zeiss EM 902 transmission electron microscope equipped with a cooled CCD digital camera (TRS, Moorenweis, Germany).

### Western blot analysis, immunoprecipitation

Protein was isolated from transfected HEK293 cells in lysis buffer containing 50 mM Tris-HCl, 150 mM NaCl, 100 mM DTT, 0.2% Triton X-100, 5 U/ml of benzonase, and 1% protease inhibitor cocktail (Sigma-Aldrich, Taufkirchen, Germany). Prior to the addition of 1–5 μg of the primary antibody, protein lysates were precleared with protein A agarose beads (Pierce, Rockford, IL, USA). Incubation with primary antibodies was performed 3 h at 4°C, and the protein–antibody complex was immobilized by the addition of 25 μl of protein A agarose beads for 1 h at 4°C. The beads were washed in PBS, and then boiled in 1× loading sample buffer for Western blot analysis using 10% SDS-PAGE. The protein was transferred to a polyvinylidene difluoride membrane (GE Healthcare, Munich, Germany) using semidry transfer (Bio-Rad, Munich, Germany). Membranes were incubated with first antibodies (dilution from 1:500 to 1:1000) overnight at 4°C. Proteins were visualized using a horseradish peroxidase (HRP)-conjugated secondary antibody (dilution 1:10,000) and ECL detection kit (GE Healthcare); the protein bands were detected by FujiFilm LAS-3000 (FujiFilm, Tokyo, Japan).

### Immunocytochemistry

HEK293 cells were grown on glass coverslips and washed 3 times in PBS. Cells were fixed with methanol at −20°C for 5 min and incubated with primary antibodies at 4°C overnight. Monoclonal rabbit anti-mouse TMEM16A antibody was used as first antibody. For immunofluorescence, cells were incubated with secondary AlexaFluor 488 goat anti-rabbit IgG for 1 h at room temperature and counterstained with Hoe33342 (Sigma-Aldrich). Immunofluorescence was detected using an Axiovert 200 microscope equipped with an ApoTome and AxioVision software (Carl Zeiss).

### Materials and statistical analysis

All compounds [ionomycin, 1-ethyl-2-benzimidazolinone (1-EBIO), riluzole, cytochalasin D, BIM, dynasore, okadaic acid, phalloidin, STO-609, KN93, KN62, KT5720, IBMX, forskolin, trifluoroperazine, calmodulin, ATP, BAPTA-AM, U0126, apyrase, and dasatinib] were from Sigma-Aldrich or Merck (Darmstadt, Germany). Peptides were synthesized by Davids Biotechnologie (Regensburg, Germany); sequences are as follows: CAM-BD 1, $NH_2$-VRKYFGEKVGLYFA-COOH; CAM-BD 2, $NH_2$-LLSKRRKCGKYGITSLLA-COOH. AO1 was generously provided by Sygnature Chemical Services Ltd. (Nottingham, UK). The anti-hTMEM16A was a generous gift from Prof. van de Rijn (Department of Pathology, Stanford University, Stanford, CA, USA). All cell culture reagents were from Gibco/Invitrogen. Student's *t* test (for paired or unpaired samples as appropriate) and ANOVA were used for statistical analysis. Values of $P < 0.05$ were accepted as significant.

## RESULTS

### TMEM16A is strictly membrane localized and is regulated by cytoskeletal components

It is believed that $Ca^{2+}$-dependent $Cl^-$ currents are activated through an increase in intracellular $Ca^{2+}$ and binding to TMEM16A or an associated protein. However, this has not been proven, and alternatively, the current may be activated by exocytosis of TMEM16A and insertion into the plasma membrane. This has been proposed for the exocrine pancreas (23). We examined localization of TMEM16A when overexpressed in HEK293 and Cos-7 cells, using immunocytochemistry and electron microscopy. TMEM16A appeared clearly membrane localized in immunohistochemistry of HEK293 cells (**Fig. 1*A***). This was confirmed by high-resolution electron microscopy using ReAsH labeling (see Materials and Methods). The images clearly indicate a strict membrane localization of TMEM16A in overexpressing HEK293 cells (Fig. 1*B*). No ReAsH labeling was observed in mock-transfected control cells (Fig. 1*C*). Similar staining was observed in Cos-7 cells after expression of TMEM16A (Supplemental Fig. S1).

Activation of TMEM16A in HEK293 cells was examined using whole-cell patch-clamp recordings. We expressed both human and mouse TMEM16A, which produced similar whole-cell $Cl^-$ conductances. While no currents were observed in HEK293 control cells, large whole-cell $Cl^-$ currents were activated by the $Ca^{2+}$ ionophore ionomycin (1 μM) in TMEM16A-expressing cells (Fig. 1*D*, *E*). Notably, whole-cell baseline currents were enhanced in TMEM16A-expressing cells, even in the absence of ionomycin, and both enhanced baseline conductance and ionomycin-activated conductance were inhibited by 10 μM AO1, a specific inhibitor of $Ca^{2+}$-activated $Cl^-$ currents (24) (Fig. 1*G*). Interestingly, activation of currents was suppressed by depolymerizing or stabilizing actin with cytochalasin D and phalloidin, respectively (Fig. 1*F*, *G*). Maneuvers that inhibit exocytosis or endocytosis (10 μM dynasore; 10 μM calmodulin-dependent kinase inhibitor STO-609; siRNA for synapsin 1) had no effect (data not shown). Thus, membrane-localized TMEM16A is activated by $Ca^{2+}$ in an actin-dependent manner.

### Phosphorylation is not a prerequisite for activation of TMEM16A

As reported earlier, intracellular N and C termini of TMEM6A carry a number of sites with consensus sequences for phosphorylation by protein kinases, such

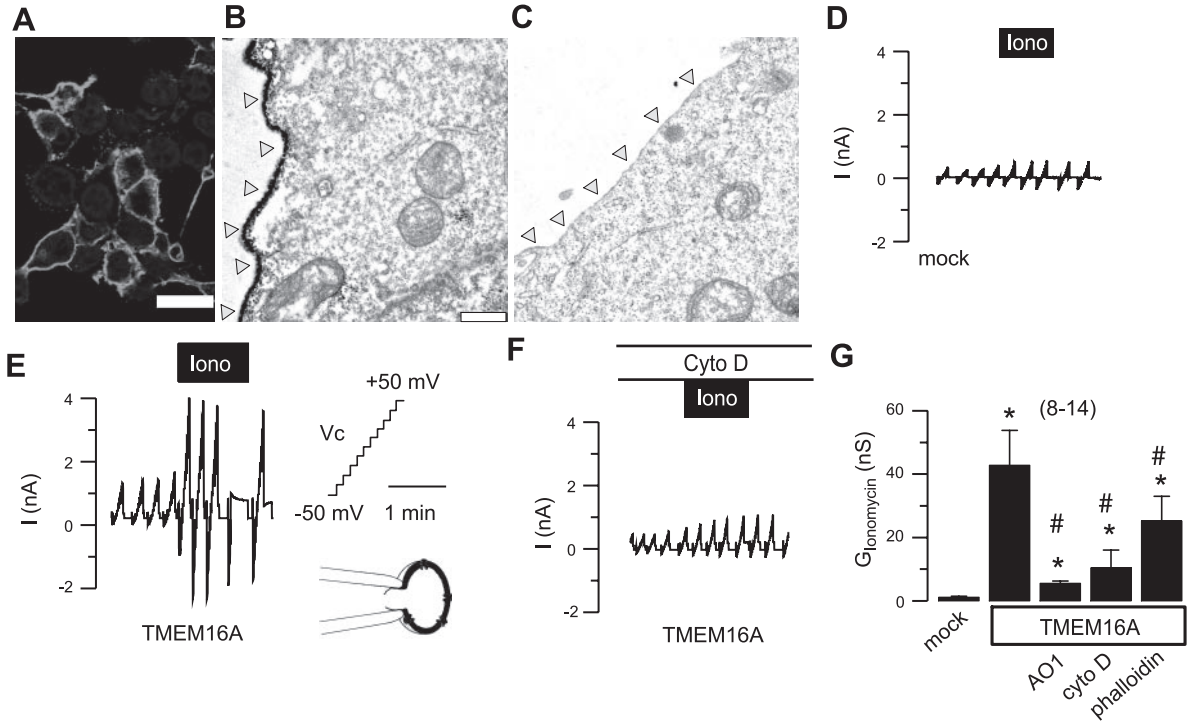


**Figure 1.** TMEM16A is strictly membrane localized and is regulated by cytoskeletal components. *A*) Immunofluorescence of TMEM16A expressed in HEK293 cells. *B*) High-resolution electron microscopy showing tetracysteine-tagged TMEM16A in HEK293 cells using ReAsH technology (triangles). *C*) Electron microscopy of mock-transfected HEK293 control cells. *D–F*) Original recordings of whole-cell currents and effects of ionomycin in mock-transfected cells (*D*) or cells overexpressing mTMEM16A before (*E*) and after (*F*) treatment with cytochalasin D (10 μM/2 h). *G*) Summary of effects of ionomycin in mock-transfected and mTMEM61A-expressing cells under control conditions and after incubation with a specific CaCC inhibitor (AO1, 10 μM), cytochalasin D (cyto D; 10 μM), and phalloidin (1 μg/ml/2 h). Cells were voltage clamped from −50 to +50 mV in steps of 10 mV. Means ± SE; $n = 8–14$. Values in parentheses indicate *n*. Scale bars = 20 μm (*A*); 500 nm (*B*). $^*P < 0.05$ for activation of whole-cell conductance by ionomycin; paired *t* test. $^{\#}P < 0.05$ *vs.* control; ANOVA.

as protein kinase A (PKA), protein kinase C (PKC), calmodulin-dependent kinase (CAMK), casein kinase 2 (CK2), and extracellular regulated kinase 1,2 (Erk1,2) (5). Moreover, the present results and a previous study suggest that cytosolic ATP is required for full activation of TMEM16A (18). Activation of TMEM16A by ionomycin (1 μM) or stimulation of P2Y receptors with ATP (100 μM) was unaffected in the presence of an ATP-free pipette filling solution ($\Delta G_{Iono}$=45±5.2 nS; $\Delta G_{ATP}$=50±5.7 nS), but it was abolished with apyrase (2 U/ml) in the patch pipette (**Fig. 2*A–E***). This suggests that cytosolic ATP is required for complete activation of TMEM16A, and it could be required for phosphorylation of the channel. Therefore, we applied ionomycin after inhibition of various kinases for which potential phosphorylation sides have been detected in TMEM16A. Cells were stimulated in the presence of inhibitors of CAMKII (KN93, KN62), PKC (BIM), PKA (KT5720), or CK2 (TBB), or in the presence of IBMX and forskolin, which increase intracellular cAMP (Fig. 2*B*). None of these treatments changed activation of TMEM16A by ionomycin. In contrast, the CAMKII inhibitor KN62 even augmented $Ca^{2+}$-activated $Cl^-$ currents, similar to

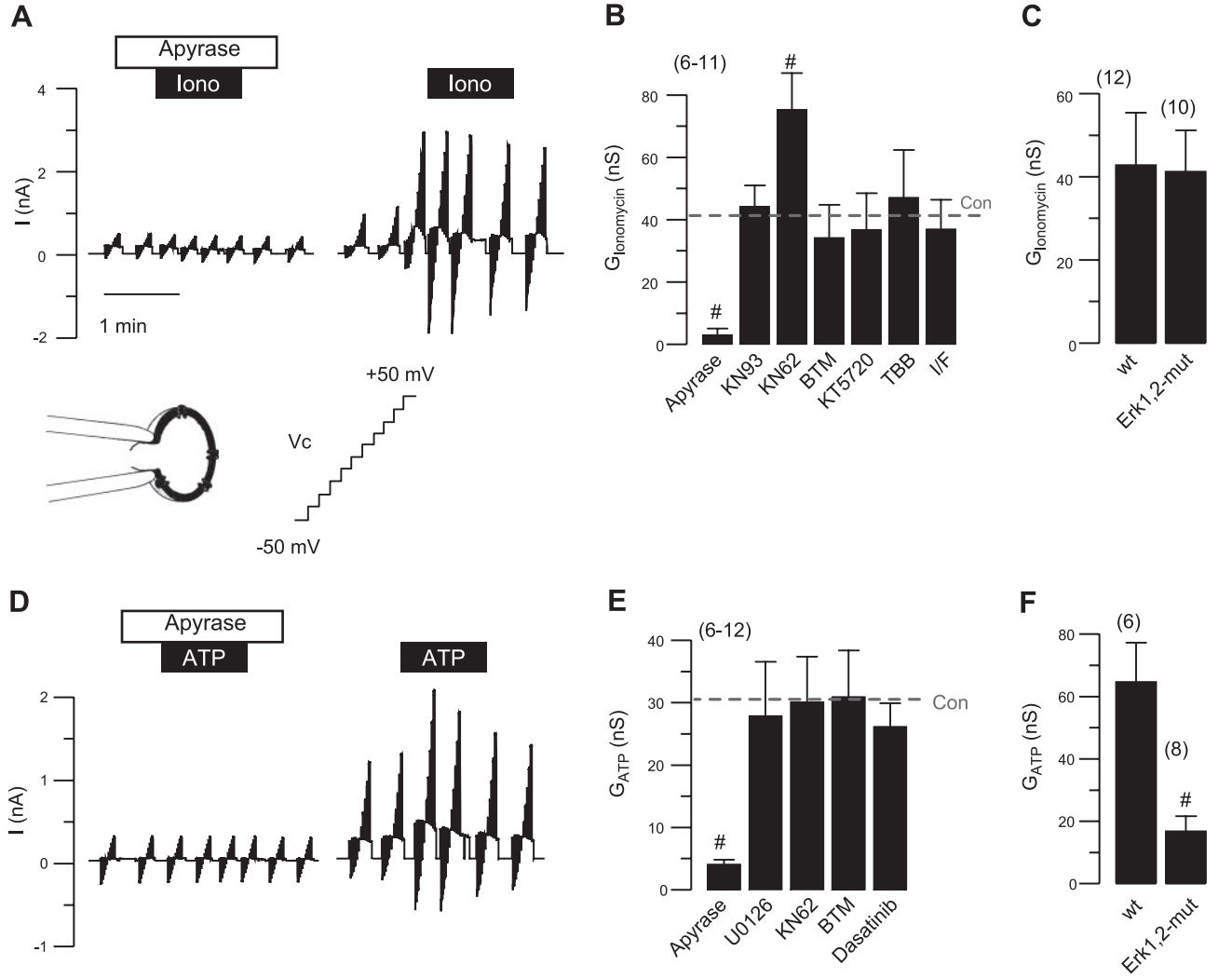


**Figure 2.** Activation of mTMEM16A requires ATP but not phosphorylation by protein kinases. *A, D*) Original recordings of whole-cell currents activated by ionomycin (1 μM; *A*) or ATP (10 μM; *D*) in mTMEM16A-expressing HEK293 cells, in the presence or absence of apyrase in the patch pipette. *B*) Summary of whole-cell conductances activated by ionomycin in the presence of apyrase (1 U/ml), after inhibition of CAMKII by KN93 (10 μM) or KN62 (10 μM) or after incubation with BIM (1 μM; inhibition of PKC), KT5720 (10 μM; inhibition of PKA), TBB (10 μM; inhibition of CK2), and stimulation with IBMX/forskolin (I/F, 100 μM/2 μM; activation of PKA). Dashed line indicates activation by ionomycin under control (con) conditions (absence of inhibitors). *C*) Summary of effects of ionomycin (1 μM) on cells expressing human wild-type (wt)TMEM16A or an mTMEM16A mutant in which 2 putative Erk1,2 phosphorylation sites have been eliminated. *E*) Summary of whole-cell conductances activated by ATP (10 μM) in the presence of apyrase in the patch pipette (1 U/ml), U0126 (10 μM; inhibition of Mek1,2), KN62 (10 μM; inhibition of CAMKII), and BIM (1 μM; inhibition of PKC). Dashed line indicates activation by ionomycin under control conditions. *F*) Summary of the effects of ATP (100 μM) on cells expressing human wtTMEM16A or an hTMEM16A mutant in which 2 putative Erk1,2 phosphorylation sites have been eliminated. Cells were voltage clamped from −50 to +50 mV in steps of 10 mV. Means ± SE; $n$ = 6–14. Values in parentheses indicate $n$. $^{\#}P < 0.05$ *vs.* control or wt; ANOVA.

what has been reported for smooth muscle cells (25, 26). Moreover, the broad nonspecific kinase inhibitor staurosporine (5 μM, 2 h) and the phosphatase 2A inhibitor okadaic acid (10 nM, 2 h) had no effect on channel activation (data not shown). All inhibitors used in the present study have been demonstrated to exert their expected actions at the concentrations used in the present report: KN63 inhibited CaCCs in CFPAC cells; BIM prevented the epithelial $Na^+$ channel ENaC from inhibition by PKC; KT5720 and TBB inhibited activation of CFTR; and U0126 attenuated $P2Y_2$-induced inhibition of ENaC. Finally, siRNA knockdown of CAMKIIγ and CK2 did not inhibit TMEM16A (data not shown).

Expression of the double-mutant S967A/S970A-TMEM16A (Erk1,2-mut) that lacks two consensus sequences for Erk1,2 in the C terminus did not change activation of TMEM16A by ionomycin but reduced receptor-mediated activation by ATP (10 μM) (Fig. 2*C*, *F*). Since the MEK inhibitor U0126 did not inhibit receptor-dependent activation of TMEM16A, stimulation of $P2Y_2$ receptors may activate Erk1,2 and TMEM16A in a MEK-independent manner, (18, 27). Nonetheless, Erk1,2 phosphorylation is not absolutely essential for channel activation, as high $[Ca^{2+}]_i$ levels (application of ionomycin) activate TMEM16a in an Erk1,2-independent fashion. Typically, ion channels that are regulated by calmodulin and the cytoskeleton are often controlled by phosphatidylinositols, such as $PIP_3$ and $PIP_2$ (28). However, we found that neither siRNA knockdown of the phosphatase and tensin homologue (PTEN), which hydrolyzes $PIP_3$ to $PIP_2$, nor inhibition of the PI3-kinase by wortmannin (1 μM; $n$=8) compromised activation of TMEM16A by ionomycin (data not shown). Thus, it remains unclear how ATP is involved in regulation of TMEM16A.

### Calmodulin is essential for activation of TMEM16A

A number of studies report activation of endogenous $Ca^{2+}$-dependent $Cl^-$ currents by CAMKII (8, 29–31), However, we did not find that CAMKII is essential for activation of TMEM16A overexpressed in HEK 293 cells (Fig. 2). In contrast, when calmodulin was inhibited by trifluoperazine (10 μM) or the highly specific inhibitor J-8 (50 μM), activation of TMEM16A by both ionomycin and ATP was largely suppressed (**Fig. 3**). This calmodulin and ATP dependence of TMEM16A is reminiscent of $Ca^{2+}$-dependent KCNN4 potassium channels, which also require both factors for complete activation (32–34). Calmodulin binds to the intracellular C terminus of KCNN4 channel and acts as a $Ca^{2+}$ sensor to control channel assembly and surface expression of KCNN4 (35).

Using a Web-based prediction program (Calmodulin Target Database; Mitsu Ikura Laboratory, Ontario Cancer Institute, University of Toronto, Toronto, ON, Canada), we identified two putative calmodulin binding domains (CAM-BD1, CAM-BD2) located in the intracellular N terminus of TMEM16A (**Fig. 4*A***). In fact, calmodulin could be coimmunoprecipitated using a TMEM16A antibody, while TMEM16A was coimmunoprecipitated by a CAM antibody in lysates from TMEM16A-expressing cells (Fig. 4*B*). No coimmunoprecipitation was observed with protein A agarose beads only. TMEM16A is expressed in different splice forms, which are characterized by amino acid inserts (segments a–d) in the N terminus and the intracellular loop (Fig. 4*A*) (1). The putative CAM-BD1 overlaps with segment b of the splice form abc-TMEM16A. We expressed the different splice forms in HEK293 cells; however, coimmunoprecipitation and detection by Western blot were unsuccessful with ac-TMEM16 (data not shown), although ac-TMEM16A and abc-TMEM16A are comparably expressed at the plasma membrane (Supplemental Fig. S2*B*). To further examine the role of these putative calmodulin binding domains, we perfused the cytosol *via* the patch pipette with short peptides corresponding to the sequences of CAM-BD1 and CAM-BD2. In the presence of CAM-BP1, activation by ionomycin of human and mouse TMEM16A was inhibited, while CAM-BP2 had no effect (Fig. 4*C–E*). These results suggest that CAM-BP1 may bind to calmodulin, thereby interfering with activation of TMEM16A.

Further attempts to confirm interaction of CAM with the N terminus of TMEM16A were unsuccessful, since 2 N-terminal truncations of TMEM16A (M266-16A and M350-16A) annihilated membrane expres-

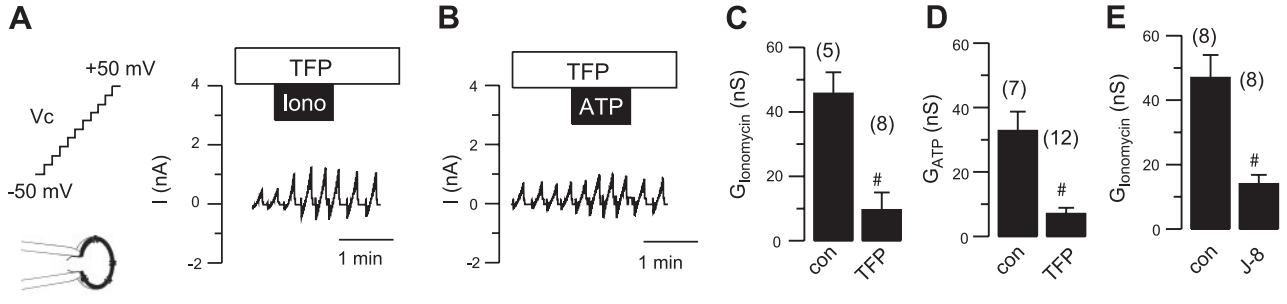


**Figure 3.** Calmodulin is essential for activation of mTMEM16A. *A*, *B*) Original recordings of whole-cell currents activated by ionomycin (Iono, 1 μM; *A*) or ATP (10 μM; *B*) in mTMEM16A expressing HEK293 cells in the presence of the CAM inhibitor trifluoperazine (TFP, 5 μM). *C–E*) Summary of whole-cell conductances activated by ionomycin (*C*, *E*) or ATP (*D*) under control conditions and in the presence of TFP (*C*, *D*) or the specific calmodulin inhibitor J-8 (50 μM; *E*). Means ± SE; $n$ = 5–12. Values in parentheses indicate $n$. $^{\#}P < 0.05$ *vs.* control; unpaired $t$ test.

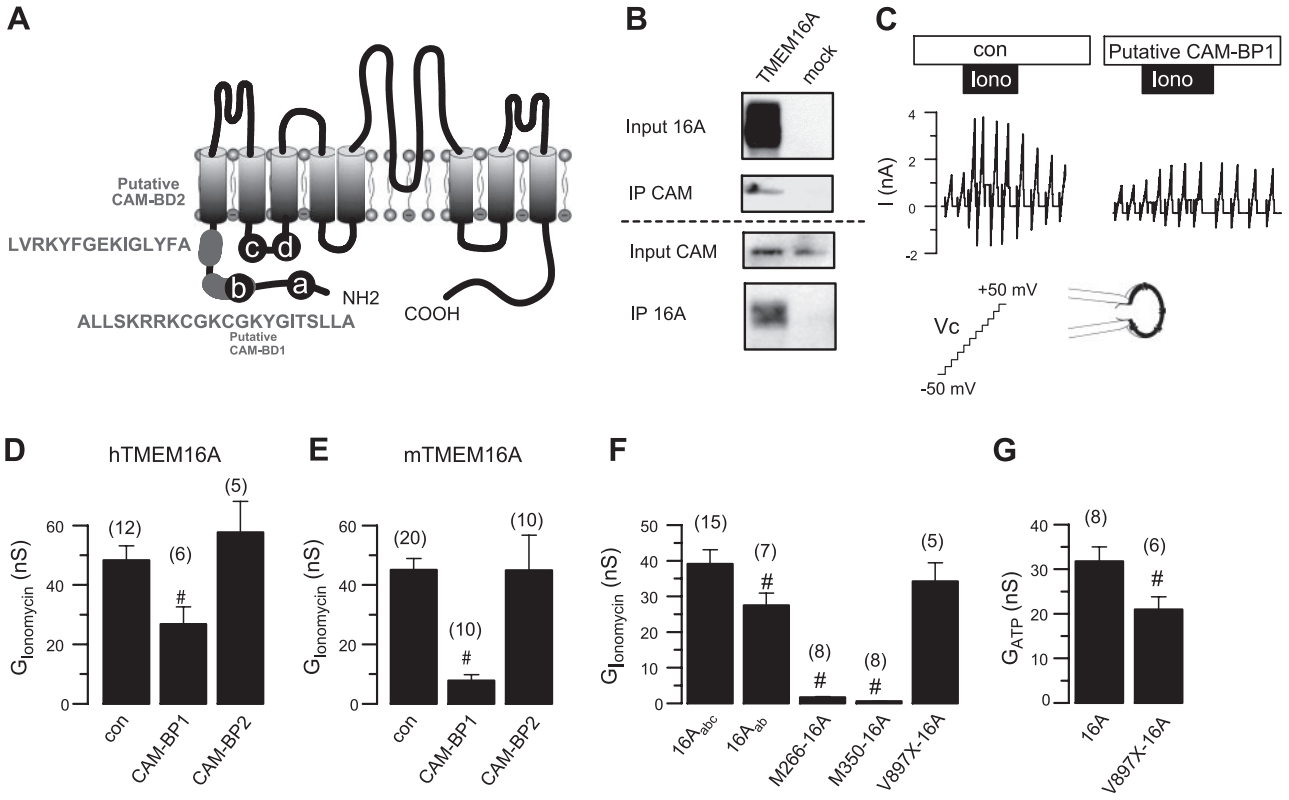


**Figure 4.** Calmodulin physically interacts with mTMEM16A and controls channel activity. *A*) N-terminal putative calmodulin binding domains CAM-BD1 and CAM-BD2 and location of the alternatively spliced sequences (*a–d*). *B*) Coimmunoprecipitation of TMEM16A and calmodulin in hTMEM16A-overexpressing HEK293 cells. Top panels: overexpressed TMEM16A (input 16A, 110 and 150 kDa; anti-hTMEM16A antibody) and coimmunoprecipitated calmodulin (IP CAM, 18 kDa; anti-hCAM antibody). Bottom panels: endogenous calmodulin expressed in HEK293 cells (input CAM; 18 kDa) and coimmunoprecipitated hTMEM16A (IP 16A; 110, and 150 kDa). *C*) Activation of whole-cell currents by ionomycin (iono; 1 μM) in hTMEM16A-expressing HEK293 cells in the absence or presence of a peptide with the amino acid sequence of the putative calmodulin binding domain CAM-BP1 in the patch pipette filling solution. *D, E*) Summary of the ionomycin-activated whole-cell conductances in human (*D*) or mouse (*E*) TMEM16A-expressing HEK293 cells. CAM-BP1 but not CAM-BP2 inhibited activation of whole-cell conductances by ionomycin. *F*) Summary of ionomycin-activated whole-cell conductances in cells expressing the splice forms abc-TMEM16A or ac-TMEM16A ($16A_{abc}$, $16A_{ac}$) or N- and C-terminal truncations of hTMEM16A (M266-16A, M350-16A, V897X-16A). *G*) Summary of ATP-activated whole-cell conductances in cells expressing wtTMEM16A or C-terminally truncated V897X-TMEM16A. Cells were voltage clamped from −50 to +50 mV in steps of 10 mV. Means ± SE; $n = 5–20$. Values in parentheses indicate *n*. con, control. $^{\#}P < 0.05$; ANOVA.

sion of the protein (Fig. 4*F* and Supplemental Fig 2*A*). Notably, truncation of the C terminus had no effect on channel activation by ionomycin, but attenuated receptor-mediated activation by ATP, probably due to elimination of the Erk1,2 sites (Fig. 4*F, G*). When we expressed the splice form ac-TMEM16A, we found that a $Cl^-$ current was still activated by ionomycin, albeit the whole-cell conductance was slightly attenuated when compared to abc-TMEM16A. Thus, the putative CAM-BD1 supports $Ca^{2+}$-dependent activation of the channel, but it is not essential for the function of TMEM16A (Fig. 4*F*).

### TMEM16A requires $Ca^{2+}$, ATP, and calmodulin for full activation

In cell-attached patches of TMEM16A-expressing HEK293 cells, we detected activation of current noise after purinergic stimulation with ATP, which was not observed in control (mock-transfected) cells (**Fig. 5*A***). However, we were unable to resolve single-channel activity, probably due to the very small single-channel conductance. When membrane patches were excised inside-out after stimulation of TMEM16A-expressing cells, the channel noise disappeared within seconds, and removal of $Ca^{2+}$ from the bath (cytosolic side) had no effect (Fig. 5*B*, top trace). In contrast to TMEM16A, $Ca^{2+}$-dependent $K^+$ channels (KCNN4, SK4) were readily detectable in excised inside-out patches and were inhibited by removal of cytosolic $Ca^{2+}$ (Fig. 5*B*, bottom trace). We measured the conductance of excised membrane patches from ATP-stimulated and TMEM16A-expressing cells immediately after excision, and 1 or 2 min after removal from the whole cell. When excised into $Ca^{2+}$-free Ringer solution, the membrane conductance of the patch was small right after excision (Fig. 5*C*). In contrast, when excised into a $Ca^{2+}$-containing Ringer solution, an outwardly rectifying current was detected that inactivated within a minute after excision, suggesting rapid rundown of TMEM16A currents (Fig. 5*D*).

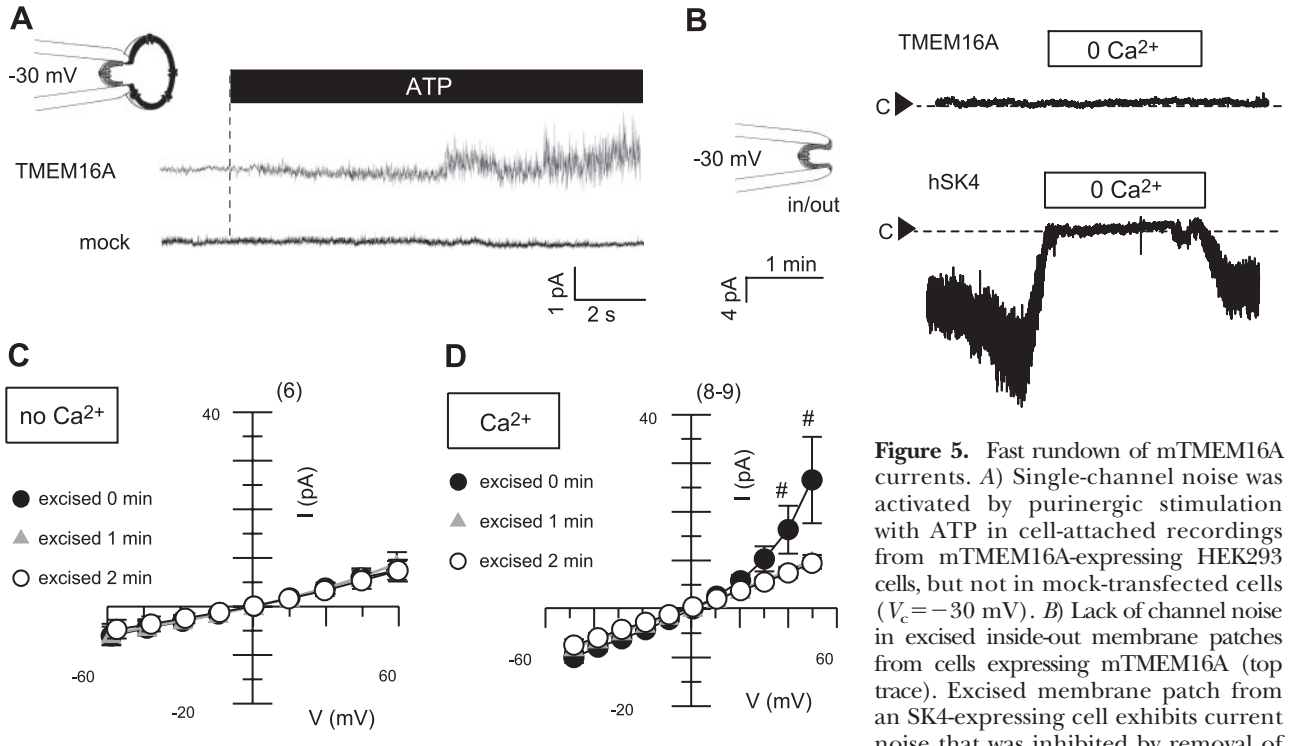


**Figure 5.** Fast rundown of mTMEM16A currents. *A*) Single-channel noise was activated by purinergic stimulation with ATP in cell-attached recordings from mTMEM16A-expressing HEK293 cells, but not in mock-transfected cells ($V_c = -30$ mV). *B*) Lack of channel noise in excised inside-out membrane patches from cells expressing mTMEM16A (top trace). Excised membrane patch from an SK4-expressing cell exhibits current noise that was inhibited by removal of $Ca^{2+}$ from the bath solution (cytosolic side). *C, D*) Current-voltage relationships obtained from membrane patches at different time points after excision into a $Ca^{2+}$-free bath solution (*C*), or bath solution containing 1 mM $Ca^{2+}$ (*D*). An outwardly rectifying current is observed immediately after excision into $Ca^{2+}$-containing bath solution (*D*) that quickly inactivated. Cells were voltage clamped from −50 to +50 mV in steps of 10 mV. Means ± SE; $n = 6–9$. Values in parentheses indicate *n*. $^{\#}P < 0.05$; unpaired *t* test.

We speculated that cytosolic factors, such as ATP or calmodulin, might get lost during membrane excision and therefore added ATP (3 mM) to the bath solution (cytosolic side), which increased the current noise and slightly enhanced the conductance of patches from TMEM16A-expressing cells, but not from mock-transfected cells (**Fig. 6**). Further addition of calmodulin (1 μg/ml) increased the channel noise and activated a membrane conductance in patches from TMEM16A-expressing cells but not from control cells. Thus ATP and calmodulin may be required to keep TMEM16A channels active (Fig. 6).

### TMEM16A and SK4 share pharmacological properties

Benzimidazolinones such as 1-EBIO are well-known activators of $Ca^{2+}$-dependent $K^+$ channels and enhance the affinity of $K^+$ channels for $Ca^{2+}$/calmodulin (36, 37). Since both SK4 and TMEM16A require CAM

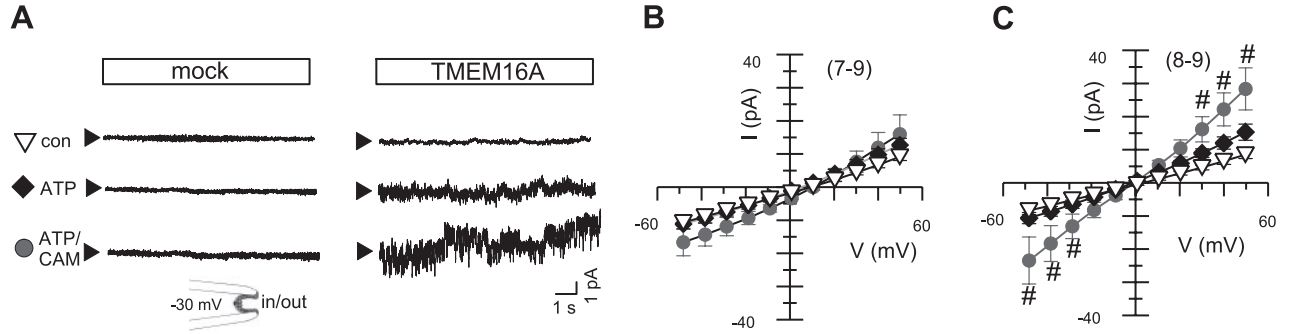


**Figure 6.** Activation of mTMEM16A requires ATP and calmodulin. *A*) Current recordings in inside-out excised membrane patches from TMEM16A and mock-transfected HEK293 cells ($V_c = +30$ mV). Current noise was small after excision of the patch in a $Ca^{2+}$-containing bath solution (con), but it was activated in excised patches from mTMEM16A-expressing cells by adding ATP (3 mM) or calmodulin (1 μg/ml) together with ATP to the cytosolic side (right panel). In contrast, no current is activated in an excised membrane patch from a mock-transfected cell (left panel). *B, C*) Current-voltage relationships measured in excised membrane patches obtained from mock-transfected (*B*) and mTMEM16A-expressing (*C*) cells, indicating current activation by ATP and calmodulin in mTMEM16A-expressing cells. Cells were voltage clamped from −50 to +50 mV in steps of 10 mV. Means ± SE; $n = 7–9$. Values in parentheses indicate *n*. $^{\#}P < 0.05$; unpaired *t* test.

and ATP to be activated, we examined whether benzimidazolinone compounds are also able to activate TMEM16A. In excised mouse tracheas, 1-EBIO (50 μM) activated a small and rather steady $Cl^-$ secretion and augmented ATP-activated short-circuit currents, apparently by activating both luminal TMEM16A and basolateral SK4 channels (**Fig. 7*A*, *B***). Notably, in the presence of the CFTR inhibitor $CFTR_{inh}172$ (5 μM), 1-EBIO still augmented ATP-induced $Cl^-$ secretion (Fig. 7*B*). In whole-cell patch-clamp experiments with human airway epithelial (Calu-3) cells, 1-EBIO and the related compound S0011198 increased whole-cell currents. However, in these cells, SK4 channels were activated by the benzimidazolones and hyperpolarized the membrane voltage, since Calu-3 cells do not express TMEM16A and do not have CaCCs (5) (Fig. 7*C*, *D* and Supplemental Fig. S3*C*). When expressed in HEK293 cells, TMEM16A was activated by 1-EBIO (50 μM) and riluzole (50 μM), another known opener of SK4 channels (38). Moreover, the related compound 5,6-dichloro-1-ethyl-1,3-dihydro-2*H*benzimidazol-2-one (DCEBIO; 1 μM) also activated TMEM16A ($\Delta G$=23.1±4.2 nS; $n$=5). In summary, both luminal $Ca^{2+}$-activated TMEM16A and basolateral SK4 $K^+$ channels are activated by the same compounds. Therefore, benzimidazolinones may be ideal drugs for the treatment of the lung disease CF, which is characterized by defective CFTR-dependent $Cl^-$ secretion and dehydration of the airways (39–41).

## DISCUSSION

### Activation of membrane-localized TMEM16A

In the present study, we examined the mechanisms for activation of the novel $Ca^{2+}$-activated $Cl^-$ channel TMEM16A and identified pharmacological properties that allow interfering with the activity of this highly relevant channel. The data demonstrate that TMEM16A is membrane localized and is activated by $Ca^{2+}$ in an actin-dependent manner. Notably, a contribution of the actin cytoskeleton to activation of endogenous CaCCs in epithelial cells has been suggested earlier (42). We found no evidence for a role of exocytosis in activating TMEM16A, and thus confirm earlier data from pancreatic acinar cells, showing exocytosis-independent activation of ion channels due to spatial distribution of cytosolic $Ca^{2+}$ (43). Similar to other epithelial ion channels, anchoring of TMEM16A to the cytoskeleton and to membrane $PIP_2$ may be essential to maintain channel activity (44, 45). A regulatory link between endogenous CaCCs, actin cyto-

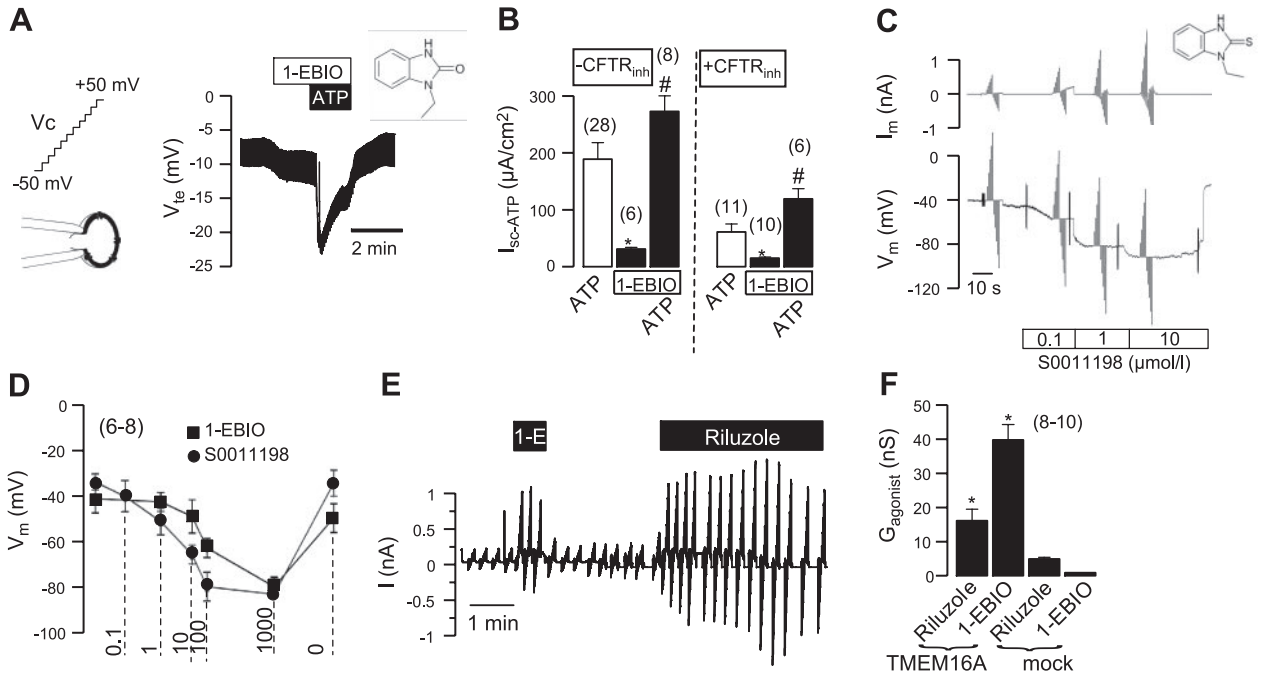


**Figure 7.** Pharmacological activation of TMEM16A and SK4 channels. *A*) Transepithelial voltage measured in Ussing chamber recordings from mouse trachea. 1-EBIO (1 mM) increases transepithelial voltage and augments subsequent negative voltage deflection induced by application of luminal ATP (100 μM). *B*) Summary of the calculated equivalent short-circuit currents activated by ATP, 1-EBIO, or simultaneous application of both. ATP-activated transport was significantly enhanced by 1-EBIO. Even after inhibition of CFTR $Cl^-$ channels by the compound $CFTR_{inh}172$ ($CFTR_{inh}$; 5 μM), 1-EBIO still augmented ATP-induced $Cl^-$ secretion. *C*) Activation of whole-cell currents and hyperpolarization of the membrane voltage of Calu3 cells by different concentrations of the homologue of 1-EBIO, S0011198. *D*) Comparison of the concentration-dependent hyperpolarizing effects of 1-EBIO and S0011198 in Calu-3 cells. *E*) Activation of whole-cell currents by 1-EBIO (1 μM) and riluzole (50 μM) in mTMEM16A-expressing HEK293 cells. *F*) Summary of the whole-cell conductances activated by 1-EBIO and riluzole in mTMEM16A-expressing HEK293 cells. Cells were voltage clamped from −50 to +50 mV in steps of 10 mV. Means ± SE; $n$ = 6–28. *$P < 0.05$ for augmentation of currents by 1-EBIO and riluzole; paired $t$ test. #$P < 0.05$ for augmentation of ATP effect by 1-EBIO; unpaired $t$ test.

skeleton, and actin-bound annexin IV has been detected earlier in colonic carcinoma cells (29).

### CAMKII, calmodulin, and ATP

Initial studies demonstrated activation of TMEM16A by an increase in cytosolic $Ca^{2+}$, but they did not present evidence for a requirement of cytosolic ATP (2, 3). We found that the presence of the ATP-cleaving enzyme apyrase in the pipette solution largely reduced channel activity, suggesting a requirement of ATP for full activation of TMEM16A. Some properties of TMEM16A are clearly different from those found for endogenous CaCCs in epithelial cells. First, TMEM16A expressed in HEK293 and FRT cells (6) is partially active at basal intracellular $Ca^{2+}$ concentrations, while endogenous CaCCs are closed under control conditions. Second, CAMKII inhibited TMEM16A currents expressed in HEK293 cells, but it activates endogenous CaCCs in colonic, airway, and pancreatic epithelial cells (8, 29–31). Notably, regulation of CaCCs by CAMKII is cell-type dependent, and inhibition of CaCCs by CAMKII has been described for smooth muscle cells (25, 26). Preliminary experiments also indicate that overexpressed TMEM16A is inhibited by CAMKII, while activation of endogenous CaCCs in CFPAC-1 cells is CAMKII dependent (data not shown). However, CFPAC-1 cells express TMEM16A endogenously, and siRNA knockdown of TMEM16A inhibits CaCCs, indicating that TMEM16A is a crucial component of the endogenous CaCCs. It is, therefore, likely that the cellular environment and/or additional auxiliary proteins determine CAMKII-dependent regulation (5).

The present data demonstrate that calmodulin is one of the auxiliary proteins necessary for activation of TMEM16A. According to the present data, the putative site for calmodulin binding overlaps with segment b of the splice form abc of TMEM16A (Fig. 4*A*). We found reduced activity of ac-TMEM16A compared with abc-TMEM16A, which is actually different from the results of a previous study (4). This discrepancy remains unexplained. However, in preliminary experiments, we found that intracellular $Ca^{2+}$ itself triggers inactivation of the channel, and inactivation of ac-TMEM16A occurs at lower $[Ca^{2+}]_i$ than for abc-TMEM16A (unpublished data). Also, it appears possible that $Ca^{2+}$ and calmodulin have more than one binding site. In overexpressing cells, additional accessory proteins may still be missing to produce a "complete" chloride channel complex. In preliminary experiments, we performed 2-hybrid screening using the split ubiquitin system in order to identify additional interacting partners, and identified the $Ca^{2+}$-binding protein S100A11. However siRNA knockdown of S100/A11 did not change TMEM16A currents.

### Similar mechanisms for activation of SK4 and TMEM16A

Calmodulin regulation of TMEM16A is reminiscent of $Ca^{2+}$/calmodulin-dependent regulation of SK4 (KCNN4) potassium channels. The open probability of SK4/IK1 channels is tightly regulated by cytosolic $Ca^{2+}$ concentrations in the range between 100 and 1000 nM, although typical $Ca^{2+}$ binding domains are not present in SK4. The pronounced $Ca^{2+}$ sensitivity of SK4 is due to its high affinity for calmodulin (32–34, 46–49). Activation of SK4/IK1 by the benzimidazolinone 1-EBIO is well established and is due to enhanced $Ca^{2+}$ sensitivity of the CAM/SK4 channel complex (37, 50–52). 1-EBIO has also been shown to activate apical $Cl^-$ channels of unknown molecular identity in rabbit conjunctival epithelium and intestinal epithelium (53, 54). However most studies claim that activation of $Cl^-$ secretion by 1-EBIO is indirect, by increasing the driving force due to activation of basolateral SK4 channels (50, 55). In this regard, a derivative of 1-EBIO, DCEBIO, was very potent in activating $K^+$ channels and on top activated an unknown apical membrane $Cl^-$ conductance in monolayers of $T_{84}$ colonic carcinoma cells (56).

We found that 1-EBIO, DCEBIO, and riluzole activated TMEM16A. An exciting finding was that only low concentrations of these compounds were required to activate TMEM16A (Supplemental Fig. S3). While typically 0.1–1 mM of 1-EBIO is required to activate SK4, TMEM16A was activated at concentrations as low as 1 μM. Despite the complex $Ca^{2+}$-dependent regulation of TMEM16A outlined above, activation by 1-EBIO, DCEBIO, and riluzole was robust and was observed for overexpressed TMEM16A as well as endogenous CaCCs in CFPAC-1 cells (Supplemental Fig. S3).

Since benzimidazolinones activate both basolateral SK4 and luminal TMEM16A channels, they could be ideal compounds for the treatment of the lung disease CF. As cAMP-dependent $Cl^-$ secretion is defective in CF, $Ca^{2+}$-dependent $Cl^-$ secretion may compensate for the defect in CFTR-function. It will be exciting to search for more potent activators of both TMEM16A and SK4. Since pharmacological properties of $Ca^{2+}$-activated $Cl^-$ and $K^+$ channels appear to overlap considerably (57), it will also be interesting to learn whether pharmacological properties of TMEM16A are altered by factors such as CAMKII, ATP, or histidine-phosphorylation, as described for SK4 channels (59, 59). As TMEM16A is broadly expressed in a number of tissues, it may become a highly relevant drug target in the future. FJ

This study was supported by the Deutsche Forschungsgemeinschaft (DFG SFB699 A7), German Mukoviszidose eV, and the EU TargetScreen2 project (EU-FP6-2005-LH-037365). The authors thank Christine Meese and Karin Schadendorf for their excellent technical support in performing the ReAsH analysis of TMEM16A. The authors thank Hoechst/Aventis for providing the benzimidazolinone compound S0011198.

## REFERENCES

1. Caputo, A., Caci, E., Ferrera, L., Pedemonte, N., Barsanti, C., Sondo, E., Pfeffer, U., Ravazzolo, R., Zegarra-Moran, O., and Galietta, L. J. (2008) TMEM16A, a membrane protein associated

with calcium-dependent chloride channel activity. *Science* **322,** 590–594
2. Schroeder, B. C., Cheng, T., Jan, Y. N., and Jan, L. Y. (2008) Expression cloning of TMEM16A as a calcium-activated chloride channel subunit. *Cell* **134,** 1019–1029
3. Yang, Y. D., Cho, H., Koo, J. Y., Tak, M. H., Cho, Y., Shim, W. S., Park, S. P., Lee, J., Lee, B., Kim, B. M., Raouf, R., Shin, Y. K., and Oh, U. (2008) TMEM16A confers receptor-activated calcium-dependent chloride conductance. *Nature* **455,** 1210–1215
4. Ferrera, L., Caputo, A., Ubby, I., Bussani, E., Zegarra-Moran, O., Ravazzolo, R., Pagani, F., and Galietta, L. J. (2009) Regulation of TMEM16A chloride channel properties by alternative splicing. *J. Biol. Chem.* **284,** 33360–33368
5. Kunzelmann, K., Kongsuphol, P., AlDehni, F., Tian, Y., Ousingsawat, J., Warth, R., and Schreiber, R. (2009) Bestrophin and TMEM16-Ca2$^+$ activated Cl$^-$ channels with different functions. *Cell Calcium* **46,** 233–241
6. Schreiber, R., Uliyakina, I., Kongsuphol, P., Warth, R., Mirza, M., Martins, J. R., and Kunzelmann, K. (2010) Expression and function of epithelial anoctamins. *J. Biol. Chem.* **285,** 7838–7845
7. Eggermont, J. (2004) Calcium-activated chloride channels: (un)known, (un)loved? *Proc. Am. Thorac. Soc.* **1,** 22–27
8. Hartzell, H. C., Putzier, I., and Arreola, J. (2005) Calcium-activated chloride channels. *Annu. Rev. Physiol.* **67,** 719–758
9. Ousingsawat, J., Martins, J. R., Schreiber, R., Rock, J. R., Harfe, B. D., and Kunzelmann, K. (2009) Loss of TMEM16A causes a defect in epithelial $Ca^{2+}$ dependent chloride transport. *J. Biol. Chem.* **284,** 28698–28703
10. Rock, J. R., O'Neal, W. K., Gabriel, S. E., Randell, S. H., Harfe, B. D., Boucher, R. C., and Grubb, B. R. (2009) Transmembrane protein 16A (TMEM16A) is a $Ca^{2+}$ regulated Cl$^-$-secretory channel in mouse airways. *J. Biol. Chem.* **284,** 14875–14880
11. Romanenko, V. G., Catalan, M. A., Brown, D. A., Putzier, I., Hartzell, H. C., Marmorstein, A. D., Gonzalez-Begne, M., Rock, J. R., Harfe, B. D., and Melvin, J. E. (2010) Tmem16A encodes the $Ca^{2+}$-activated Cl$^-$ channel in mouse submandibular salivary gland acinar cells. *J. Biol. Chem.* **285,** 12990–13001
12. Lee, R. J., and Foskett, J. K. (2009) Mechanisms of $Ca^{2+}$-stimulated fluid secretion by porcine bronchial submucosal gland serous acinar cells. *Am. J. Physiol. Lung Cell. Mol. Physiol.* **298,** L210–L231
13. Rock, J. R., Futtner, C. R., and Harfe, B. D. (2008) The transmembrane protein TMEM16A is required for normal development of the murine trachea. *Dev. Biol.* **321,** 141–149
14. Gomez-Pinilla, P. J., Gibbons, S. J., Bardsley, M. R., Lorincz, A., Pozo, M. J., Pasricha, P. J., van de, R. M., West, R. B., Sarr, M. G., Kendrick, M. L., Cima, R. R., Dozois, E. J., Larson, D. W., Ordog, T., and Farrugia, G. (2009) Ano1 is a selective marker of interstitial cells of Cajal in the human and mouse gastrointestinal tract. *Am. J. Physiol. Gastrointest. Liver Physiol.* **296,** G1370–G1381
15. Huang, F., Rock, J. R., Harfe, B. D., Cheng, T., Huang, X., Jan, Y. N., and Jan, L. Y. (2009) Studies on expression and function of the TMEM16A calcium-activated chloride channel. *Proc. Natl. Acad. Sci. U. S. A.* **106,** 21413–21418
16. Hwang, S. J., Blair, P. J., Britton, F. C., O'Driscoll, K. E., Hennig, G., Bayguinov, Y. R., Rock, J. R., Harfe, B. D., Sanders, K. M., and Ward, S. M. (2009) Expression of anoctamin 1/TMEM16A by interstitial cells of Cajal is fundamental for slow wave activity in gastrointestinal muscles. *J. Physiol.* **587,** 4887–4904
17. Liu, B., Linley, J. E., Du, X., Zhang, X., Ooi, L., Zhang, H., and Gamper, N. (2010) The acute nociceptive signals induced by bradykinin in rat sensory neurons are mediated by inhibition of M-type $K^+$ channels and activation of Ca2$^+$-activated Cl$^-$ channels. *J. Clin. Invest.* **120,** 1240–1252
18. Almaca, J., Tian, Y., AlDehni, F., Ousingsawat, J., Kongsuphol, P., Rock, J. R., Harfe, B. D., Schreiber, R., and Kunzelmann, K. (2009) TMEM16 proteins produce volume regulated chloride currents that are reduced in mice lacking TMEM16A. *J. Biol. Chem.* **284,** 28571–28578
19. Skals, M., Jensen, U. B., Ousingsawat, J., Kunzelmann, K., Leipziger, J., and Praetorius, H. A. (2010) E. coli alpha-hemolysin triggers shrinkage of erythrocytes via KCa3.1 and TMEM16A channels with subsequent phosphatidyl serine exposure. *J. Biol. Chem.* **285,** 15557–15565
20. Galietta, L. J. (2009) The TMEM16 protein family: a new class of chloride channels? *Biophys. J.* **97,** 3047–3053
21. Jensen, B. S., Strobaek, D., Olesen, S. P., and Christophersen, P. (2001) The $Ca^{2+}$-activated $K^+$ channel of intermediate conductance: a molecular target for novel treatments? *Curr. Drug. Targets* **2,** 401–422
22. Ausubel, F. A., Brent, R., Kingston, R. E., Moore, D. D., Seidman, J. G., Smith, J. A., and Struhl, K., eds. (1996) *Current Protocols in Molecular Biology*, pp. 9.2.1–9.2.10, John Wiley & Sons, New York
23. Petersen, O. H., and Tepikin, A. V. (2008) Polarized calcium signaling in exocrine gland cells. *Annu. Rev. Physiol.* **70,** 273–299
24. De la Fuente, R., Namkung, W., Mills, A., and Verkman, A. S. (2007) Small molecule screen identifies inhibitors of a human intestinal calcium activated chloride channel. *Mol. Pharmacol.* **73,** 758–768
25. Greenwood, I. A., Ledoux, J., and Leblanc, N. (2001) Differential regulation of $Ca^{2+}$-activated Cl$^-$ currents in rabbit arterial and portal vein smooth muscle cells by $Ca^{2+}$-calmodulin-dependent kinase. *J. Physiol.* **534,** 395–408
26. Wang, Y. X., and Kotlikoff, M. I. (1997) Inactivation of calcium-activated chloride channels in smooth muscle by calcium/calmodulin-dependent protein kinase. *Proc. Natl. Acad. Sci. U. S. A.* **94,** 14918–14923
27. Chorna, N. E., Chevres M., Santos-Berrios C., Orellano E. A., Erb, L., and Gonzalez, F. A. (2007) P2Y2 receptors induced cell surface redistribution of alpha (v) integrin is required for activation of ERK 1/2 in U937 cells. *J. Cell. Physiol.* **211,** 410–422
28. Balla, T., Szentpetery, Z., and Kim, Y. J. (2009) Phosphoinositide signaling: new tools and insights. *Physiology* **24,** 231–244
29. Chan, H. C., Kaetzel, M. A., Gotter, A. L., Dedman, J. R., and Nelson, D. J. (1994) Annexin IV inhibits calmodulin-dependent protein kinase II-activated chloride conductance. A novel mechanism for ion channel regulation. *J. Biol. Chem.* **269,** 32464–32468
30. Ho, M. W., Kaetzel, M. A., Armstrong, D. L., and Shears, S. B. (2001) Regulation of a human chloride channel. a paradigm for integrating input from calcium, type ii calmodulin-dependent protein kinase, and inositol 3,4,5,6-tetrakisphosphate. *J. Biol. Chem.* **276,** 18673–18680
31. Wagner, J. A., Cozens, A. L., Schulman, H., Gruenert, D. C., Stryer, L., and Gardner, P. (1991) Activation of chloride chanels in normal and cystic fibrosis airway epithelial cells by multifunctional calcium/calmodulin-dependent protein kinase. *Nature* **349,** 793–796
32. Pedersen, K. A., Schroder, R. L., Skaaning-Jensen, B., Strobaek, D., Olesen, S. P., and Christophersen, P. (1999) Activation of the human intermediate-conductance $Ca^{2+}$-activated $K^+$ channel by 1-ethyl-2-benzimidazolinone is strongly $Ca^{2+}$-dependent. *Biochim. Biophys. Acta* **1420,** 231–240
33. Strobaek, D., Teuber, L., Jorgensen, T. D., Ahring, P. K., Kjaer, K., Hansen, R. S., Olesen, S. P., Christophersen, P., and Skaaning-Jensen, B. (2004) Activation of human IK and SK $Ca^{2+}$-activated $K^+$ channels by NS309 (6,7-dichloro-1H-indole-2,3-dione 3-oxime). *Biochim. Biophys. Acta* **1665,** 1–5
34. Syme, C. A., Gerlach, A. C., Singh, A. K., and Devor, D. C. (2000) Pharmacological activation of cloned intermediate- and small-conductance $Ca^{2+}$-activated $K^+$ channels. *Am. J. Physiol.* **278,** C570–C581
35. Kolb, H.-A. (1990) Potassium channels in excitable and non-excitable cells. *Rev. Physiol. Biochem. Pharmacol.* **115,** 51–91
36. Devor, D. C., Singh, A. K., Frizzell, R. A., and Bridges, R. J. (1996) Modulation of Cl$^-$ secretion by benzimidazolones. I. Direct activation of a $Ca^{2+}$-dependent $K^+$ channel. *Am. J. Physiol. Lung Cell. Mol. Physiol.* **271,** L775–L784
37. Von Hahn, T., Thiele, I., Zingaro, L., Hamm, K., Garcia-Alzamora, M., Köttgen, M., Bleich, M., and Warth, R. (2001) Characterisation of the rat SK4/IK1 $K^+$ channel. *Cell. Physiol. Biochem.* **11,** 219–230
38. Sankaranarayanan, A., Raman, G., Busch, C., Schultz, T., Zimin, P. I., Hoyer, J., Kohler, R., and Wulff, H. (2009) Naphtho[1,2-d]thiazol-2-ylamine (SKA-31), a new activator of KCa2 and KCa3.1 potassium channels, potentiates the endothelium-derived hyperpolarizing factor response and lowers blood pressure. *Mol. Pharmacol.* **75,** 281–295
39. Boucher, R. C. (2007) Evidence for airway surface dehydration as the initiating event in CF airway disease. *J. Intern. Med.* **261,** 5–16
40. Kunzelmann, K., and Mall, M. (2003) Pharmacotherapy of the ion transport defect in cystic fibrosis: role of purinergic receptor

agonists and other potential therapeutics. *Am. J. Respir. Med.* **2,** 299–309
41. Preston, P., Wartosch, L., Gunzel, D., Fromm, M., Kongsuphol, P., Ousingsawat, J., Kunzelmann, K., Barhanin, J., Warth, R., and Jentsch, T. J. (2010) Disruption of the $K^+$ channel beta-subunit KCNE3 reveals an important role in intestinal and tracheal $Cl^-$ transport. *J. Biol. Chem.* **285,** 7165–7175
42. Hug, T., Koslowsky, T., Ecke, D., Greger, R., and Kunzelmann, K. (1995) Actin-dependent activation of ion conductances in bronchial epithelial cells. *Pflügers Arch.* **429,** 682–690
43. Maruyama, Y. (1996) Selective activation of exocytosis by low concentrations of ACh in rat pancreatic acinar cells. *J. Physiol.* **492,** 807–814
44. Mazzochi, C., Benos, D. J., and Smith, P. R. (2006) Interaction of epithelial ion channels with the actin-based cytoskeleton. *Am. J. Physiol. Renal Physiol.* **291,** F1113–F1122
45. Thelin, W. R., Chen, Y., Gentzsch, M., Kreda, S. M., Sallee, J. L., Scarlett, C. O., Borchers, C. H., Jacobson, K., Stutts, M. J., and Milgram, S. L. (2007) Direct interaction with filamins modulates the stability and plasma membrane expression of CFTR. *J. Clin. Invest.* **117,** 364–374
46. Fanger, C. M., Ghanshani, S., Logsdon, N. J., Rauer, H., Kalman, K., Zhou, J., Beckingham, K., Chandy, K. G., Cahalan, M. D., and Aiyar, J. (1999) Calmodulin mediates calcium-dependent activation of the intermediate conductance KCa channel, IKCa1. *J. Biol. Chem.* **274,** 5746–5754
47. Joiner, W. J., Khanna, R., Schlichter, L. C., and Kaczmarek, L. K. (2001) Calmodulin regulates assembly and trafficking of SK4/IK1 $Ca^{2+}$-activated $K^+$ channels. *J. Biol. Chem.* **276,** 37980–37985
48. Khanna, R., Chang, M. C., Joiner, W. J., Kaczmarek, L. K., and Schlichter, L. C. (1999) hSK4/hIK1, a calmodulin-binding KCa channel in human T lymphocytes. Roles in proliferation and volume regulation. *J. Biol. Chem.* **274,** 14838–14849
49. Xia, X. M., Fakler, B., Rivard, A., Wayman, G., Johnson-Pais, T., Keen, J. E., Ishii, T., Hirschberg, B., Bond, C. T., Lutsenko, S., Maylie, J., and Adelman, J. P. (1998) Mechanism of calcium gating in small-conductance calcium-activated potassium channels. *Nature* **395,** 503–507
50. Hamilton, K. L., Meads, L., and Butt, A. G. (1999) 1-EBIO stimulates $Cl^-$ secretion by activating a basolateral $K^+$ channel in the mouse jejunum. *Pflügers Arch.* **439,** 158–166
51. Pedarzani, P., Mosbacher, J., Rivard, A., Cingolani, L. A., Oliver, D., Stocker, M., Adelman, J. P., and Fakler, B. (2001) Control of electrical activity in central neurons by modulating the gating of small conductance $Ca^{2+}$-activated $K^+$ channels. *J. Biol. Chem.* **276,** 9762–9769
52. Warth, R., Hamm, K., Bleich, M., Kunzelmann, K., vonHahn, T., Schreiber, R., Ullrich, E., Mengel, M., Trautmann, N., Kindle, P., Schwab, A., and Greger, R. (1999) Molecular and functional characterization of the small $Ca^{2+}$-regulated $K^+$ channel (rSK4) of colonic crypts. *Pflügers Arch.* **438,** 437–444
53. Alvarez, L. J., Zamudio, A. C., and Candia, O. A. (2005) Cl-secretory effects of EBIO in the rabbit conjunctival epithelium. *Am. J. Physiol. Cell Physiol.* **289,** C138–C147
54. Hamilton, K. L., and Kiessling, M. (2006) DCEBIO stimulates Cl- secretion in the mouse jejunum. *Am. J. Physiol. Cell Physiol.* **290,** C152–C164
55. Devor, D. C., Singh, A. K., Bridges, R. J., and Frizzell, R. A. (1996) Modulation of $Cl^-$ secretion by benzimidazolones. II. Coordinate regulation of apical $G_{Cl}$ and basolateral $G_K$. *Am. J. Physiol. Lung Cell. Mol. Physiol.* **271,** L785–L795
56. Singh, S., Syme, C. A., Singh, A. K., Devor, D. C., and Bridges, R. J. (2001) Benzimidazolone activators of chloride secretion: potential therapeutics for cystic fibrosis and chronic obstructive pulmonary disease. *J. Pharmacol. Exp. Ther.* **296,** 600–611
57. Saleh, S. N., Angermann, J. E., Sones, W. R., Leblanc, N., and Greenwood, I. A. (2007) Stimulation of $Ca^{2+}$-gated $Cl^-$ currents by the calcium-dependent $K^+$ channel modulators NS1619 [1,3-dihydro-1-[2-hydroxy-5-(trifluo[zhy]romethyl)phenyl]-5-(trifluoromethyl)-2H-benzi midazol-2-one] and isopimaric acid. *J. Pharmacol. Exp. Ther.* **321,** 1075–1084
58. Gerlach, A. C., Syme, C. A., Giltinan, L., Adelman, J. P., and Devors, D. C. (2001) ATP-dependent activation of the intermediate conductance, $Ca^{2+}$-activated $K^+$ channel, hIK1, is conferred by a C-terminal domain. *J. Biol. Chem.* **276,** 10963–10970
59. Wiwchar, M., Ayon, R., Greenwood, I. A., and Leblanc, N. (2009) Phosphorylation alters the pharmacology of $Ca^{2+}$-activated Cl channels in rabbit pulmonary arterial smooth muscle cells. *Br. J. Pharmacol.* **158,** 1356–1365

*Received for publication August 26, 2010.*
*Accepted for publication November 11, 2011.*